New Directions in Lifting Surface Theory

HOLT ASHLEY, SHEILA WINDALL, AND MARTEN T. LANDAHL
Massachusetts Institute of Technology, Cambridge, Mass.

Nomenclature

a = speed of sound, dimensionless
$\mathcal{AR}$ = aspect ratio of planar lifting surface
b = wing semichord, ft
b_1 = chordwise dimension of area element in supersonic and transonic theory
c = local wing chord, ft
c_0 = reference chordlength, ft
C_L $\equiv 2L/\rho_\infty U^2 S$ = lift coefficient
C_M = coefficient of pitching moment
C_p = $(p - p_\infty)/(\rho_\infty \mu^2/2)$ = pressure coefficient
d = depth of x-y plane below free liquid surface, ft or dimensionless
D = depth below free surface, referred to l
F $\equiv U/(gl)^{1/2}$ = Froude number
g = gravitational constant, ft/sec^2
h = height of wing midspan above ground plane, ft; also downward bending or heaving displacement, ft
h_0 = reference value of bending displacement at wingtip
i $\equiv (-1)^{1/2}$ = complex unit
k $\equiv \omega k/U$ or $\omega l/U$ = reduced frequency
k_1 $\equiv kb_1/b$ = reduced frequency based on area-element size
K = kernel function of subsonic integral equation
l = reference length, ft
L = upward normal force or force per unit span acting on lifting surface
n, m = chordwise and spanwise coordinates of "receiving" area element, dimensionless
M = flight Mach number
p = static pressure
r = distance between points, dimensionless
R $\equiv \{(x - \xi)^2 + (1 - M^2)[(y - \eta)^2 + (z - z_0(\eta))^2]\}^{1/2}$ = elliptical distance
s, n = curvilinear coordinates measured spanwise along and normal to surface, dimensionless
$\bar{s}$ $\equiv s/s_{\text{TIP}}$ = normalized s
S = projected cylindrical lifting surface area, ft^2 or dimensionless; also spanwise distance on cantilever wing, measured in semispans.
t = time coordinate, sec
u, v, w = fluid velocity components, dimensionless
U = flight speed, fps
v_n = velocity component normal to S, dimensionless
W = function describing wake surface
x, y, z = rectangular Cartesian coordinates, dimensionless, see Fig. 1
$z_0(y)$ = height of S above x-y plane, dimensionless
Δz = displacement of wing above its projected surface, dimensionless
α = angle of attack measured from zero lift
β $\equiv (M^2 - 1)^{1/2}$ = cotangent of Mach angle
$\Delta(\ )$ = discontinuous jump in a quantity, passing from lower to upper surface of wing
ϵ = a small quantity, the largest of angle of attack, thickness ratio, fractional camber or amplitude ratio of unsteady motion
ξ, η, ζ = integration variables replacing x, y, z
θ $\equiv \tan^{-1}(dz_0/dy)$ = slope of S; also angle variable into which x is transformed
λ, λ_1 = dummy variables of integration
ν, μ = coordinates of "sending" area element in influence coefficient theory, dimensionless
$\bar{\nu}, \bar{\mu}$ = symbols for relative positions of "receiving" and "sending" area elements
ρ = fluid density
σ = integration variable replacing s
τ = time coordinate, dimensionless
φ $\equiv \Phi/Ul$ = perturbation potential, dimensionless; also, with various subscripts, phase angle of complex simple harmonic quantity
Φ = perturbation potential, ft^2/sec
ψ = $(p_\infty - p)/\rho_\infty U^2$ acceleration potential, dimensionless
ω = circular frequency of simple harmonic quantity, sec^{-1}

Subscripts

l = lower surface of wing
p = local value of flow property
$(\ldots)_R + i(\ldots)_I$ = real and imaginary parts of complex number
u = upper surface of wing
1 = coordinate referred to b_1
∞ = property of undisturbed fluid
$|\ |$ = magnitude of complex number
$\overline{(\ )}$ = complex amplitude of simple harmonic quantity

Introduction

ALTHOUGH theoretical investigation of the loading of lifting surfaces antedates the achievement of powered flight, efforts have been focused largely on single, almost plane configurations in steady motion. Since mathematical tractability has often been the criterion of interest, there exist numerous elegant applications of analysis to specific planform shapes and camber distributions. The extensive literature in this area need not be rehearsed here, except for drawing attention to excellent surveys such as Jones and Cohen.[1] Proportionately much less work has been devoted, on the one hand, to unsteady motions of wings and, on the other, to so-called "interference problems," i.e., loading in the vicinity of boundaries, aggregates of adjacent lifting surfaces and bodies that resemble actual flight vehicles, and the like. The bulk of published interference theory relies heavily on the slender-body simplification,[2, 3] whose limitations as a quantitative design tool are well known; moreover, other interference procedures consist mainly of unidirectional couplings between flow fields, along the lines described by Ferrari.[4]

In the era of digital computers with multiplication times of a few microseconds, it is self-evident that the powers of classical analysis should be supplemented by numerical approaches, some of which might have seemed impractical even a decade ago. It is the purpose of the present paper to review a few of these, for which various degrees of verification already exist, and to suggest ways for removing certain imperfections inherent in first-generation numerical theory for arbitrary lifting surfaces.

Presented as Preprint 64-1 at the AIAA Aerospace Sciences Meeting, New York, January 20–22, 1964; revision received July 22, 1964. This work was sponsored in part by the U. S. Navy Bureau of Ships, General Hydromechanics Research Program, S-R009 01001, technically administered by the David Taylor Model Basin under Contract Nonr-1841 (81).

Two of the authors have a long-standing concern with aeroelastic stability and dynamic-loading phenomena. The work to be described, therefore, emphasizes unsteady motion consisting of small, simple harmonic oscillations normal to the loaded surface, with steady flow included as a low-frequency limit. Under the familiar small-perturbation hypothesis, any smooth oscillatory displacement of very general classes of nearly plane wings can be represented as an integral equation over the lifting area[5] when the Mach number $M < 1$ and as a direct integration[6] when $M > 1$. For high enough values of reduced frequency, even the transonic case may be treated in a manner resembling the supersonic. What is not so well known is that similar representations can be derived for lifting systems whose projected surfaces are highly nonplanar. For instance, a T tail at subsonic speeds is describable with a pair of coupled integral equations, and a ground plane requires only a nonsingular correction to be added to the appropriate kernel function. When treated by numerical means, these problem statements lead to mathematically self-consistent numerical procedures, whose errors can be estimated and whose results can be made to converge to "exact" linearized solutions by indefinitely refining a collocation net or a quadrature formula.

One by-product of this extension to nonplanar configurations is that many earlier techniques for solving interference problems by inconsistent approximations are rendered obsolete, except for purposes of preliminary estimation. It is also worth mentioning that a convenient, systematic introduction to thin-wing theory can be made through the "inner-and-outer" method of Kaplun and Lagerstrom[7]; ordinary linearized theory coincides with the term in the outer expansion which is of first order in a small parameter ϵ, denoting the largest of the four numbers, i.e., thickness ratio, fractional camber, angle of attack, or amplitude ratio of unsteady motion. Only the simple harmonic case is analyzed here, because Fourier superposition has repeatedly proved itself as a means of dealing with time-dependent transient motion of three-dimensional surfaces.

Most of the linearized formulations given below, as well as some of the examples, have appeared in earlier papers by the authors[8-10] and others[5, 11, 12]. Brief repetition is believed to be justified in the interests of completeness and as a background for subsequent discussion of limitations and nonlinear extensions. More comprehensive citations to the literature of linearized unsteady theory are also contained in Refs. 8 and 10.

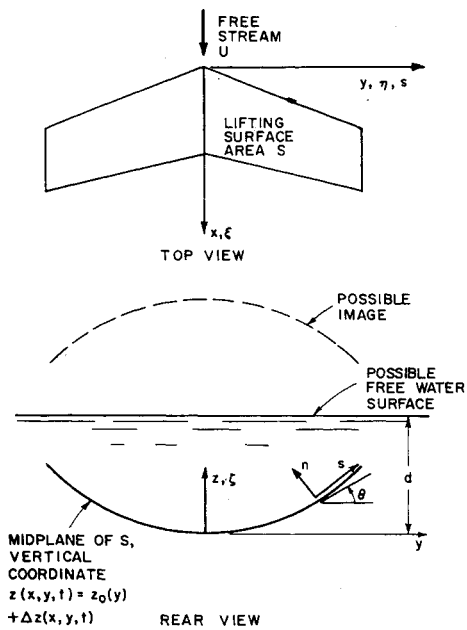

Fig. 1 Top and rear elevations of a thin, nonplanar lifting surface performing small unsteady motions normal to a uniform subsonic or supersonic stream flowing parallel to the x coordinate. The image of this wing in a ground plane or free water surface is shown.

Numerical Solution of Linearized Problems

Constant-Density and Subsonic Speeds

Consider small incidence or oscillatory displacement of a lifting surface like the one illustrated in Fig. 1. For the moment, let the free water surface or ground plane recede to infinity, and let the thickness be assumed zero, as is done in sample calculations below. When S happens to be nearly flat, thickness effects are symmetrical with respect to the x-y plane and can be treated separately from the loading problem. Decoupling is also possible during unsteady loads calculation for nonplanar wings, but it cannot be achieved in steady flow, where one must represent thickness with a superimposed source sheet that interacts with the doublets describing the lifting part of the field. This minor refinement is omitted from the present discussion.

For convenience, all spatial coordinates, such as those in Fig. 1, are made dimensionless by division with a reference length l, usually chosen to be the semichord b_0 at midspan. Velocity components are referred to flight speed U. The projected surface of the wing in Fig. 1 is the cylinder $z = z_0(y)$, and to this is added a sinusoidal displacement, given in the customary complex notation by

$$\Delta z(x, y, t) = \Delta\bar{z}(x, y)e^{i\omega t} \tag{1}$$

Flow perturbations are due to the normal displacement

$$\bar{n}(x, y)e^{i\omega t} = \Delta\bar{z}e^{i\omega t}\sec\theta(y) \tag{2}$$

which forces the fluid particles in contact with S to have the normal velocities

$$\begin{aligned} v_n(x, y, t) &= \bar{v}_n(x, s)e^{i\omega t} \\ &= [(\partial\bar{n}/\partial x) + ik\bar{n}]e^{i\omega t} \end{aligned} \tag{3}$$

Principal notation, such as the reduced frequency $k = \omega l/U$, will be found listed in the Nomenclature. The curvilinear coordinates (x, s), being single valued, are more suitable for identifying points on S than (x, y).

For subsonic flow, the dimensionless acceleration potential

$$\psi \equiv \frac{p_\infty - p}{\rho_\infty U^2} = \bar{\psi}e^{i\omega t} \tag{4}$$

is the basic dependent variable. Pressure discontinuities can occur only through S and are, therefore, represented by normally oriented doublets of ψ over this area alone. It is easily proved that the strength of such a layer is locally proportional to the discontinuity $\Delta\psi$ and hence to

$$p_l - p_u = \Delta\bar{p}(x, s)e^{i\omega t} \tag{5}$$

By a slight extension of Watkins, Runyan, and Woolston's work,[5] one can derive the following formula:

$$\bar{\psi}(x, y, z) = \iint_S \frac{\Delta\bar{p}}{4\pi\rho_\infty U^2} \times \frac{\partial}{\partial n_1}\left\{\frac{\exp ik\{[M^2(x - \xi) - MR]/(1 - M^2)\}}{R}\right\} d\xi d\sigma \tag{6}$$

where

$$R \equiv \{(x - \xi)^2 + (1 - M^2)[(y - \eta)^2 + (z - z_0(\eta))^2]\}^{1/2}$$

and (ξ, η, σ) are dummy variables replacing (x, y, s) in the wing surface, n_1 is the normal direction at point $\xi, \eta, z_0(\eta)$.

From the well-known relation between ψ and the velocity potential, one expresses the flow-tangency boundary condition in terms of the known distribution of $\bar{v}_n(x, s)$ as

$$\bar{v}_n(x, s) = e^{-ikx} \int_{-\infty}^{x} \frac{\partial \bar{\psi}}{\partial n}(x, s) e^{ik\lambda} d\lambda \quad \text{for} \quad (x, s) \text{ on } S \qquad (7)$$

Combining Eqs. (6) and (7), one is led to the principal integral equation

$$\bar{v}_n(x, s) = \iint_S \frac{\Delta \bar{p}}{4\pi \rho_\infty U^2} K d\xi d\sigma \qquad (8)$$

Here the kernel function K has the physical significance of normal velocity at (x, s) due to a unit Dirac delta function of pressure loading, acting perpendicular to the surface at (ξ, σ) in a subsonic, irrotational stream of perfect gas. The Appendix gives a formal representation of K, along with the explicit formula appropriate to constant-density flow. A number of other kernel functions, applicable to such situations as two- or three-dimensional loaded hydrofoils running beneath a free water surface, ground effect, and apparent-mass estimation, are also listed there.

With minor variations depending on the physical situation and kernel-function singularities, the solution of integral equations like Eq. (8) is conveniently carried out along lines pioneered by Watkins, Woolston, and Cunningham.[13] The distribution of Δp is approximated by a rapidly convergent series of functions which reproduce the proper leading-edge singularity, fulfill the Kutta condition along the trailing edge (if appropriate), and drop to zero with the proper infinite slope also along side edges. Integration area S is first transformed into a rectangle by

$$\begin{aligned} s &= s_{\text{TIP}} \bar{s} \\ x &= \tfrac{1}{2}[x_T(s) + x_L(s)] - \tfrac{1}{2}[x_T(s) - x_L(s)] \cos\theta \end{aligned} \qquad (9)$$

Here x_L and x_T are coordinates of the leading and trailing edges, respectively, whereas the tips are arranged to lie at $s = \pm s_{\text{TIP}}$. For each member of the system of loaded surfaces, the pressure series reads

$$\frac{\Delta \bar{p}(\theta, \bar{s})}{4\pi \rho_\infty U^2} = \frac{s_{\text{TIP}}}{b(\bar{s})} (1 - \bar{s}^2)^{1/2} \left\{ \sum_{m=0} a_{0_m} \bar{s}^m \cot \frac{\theta}{2} + \sum_{n=1} \sum_{m=0} a_{nm} \bar{s}^m \sin n\theta \right\} \qquad (10)$$

Using dummy integration variables in place of $(\theta, \bar{s})$, Eq. (10) is substituted into Eq. (8). The integrals are evaluated at a set of stations (x, s) on S, using symmetry to operate on one half-span when possible. Numerical integration must be done with care, especially to obtain the correct finite part[13] at singularities of the kernel function. This is the

---

Dr. Holt Ashley studied from 1940 to 1943 at the California Institute of Technology. While serving as a meteorologist and staff weather officer with the U. S. Army Air Force, he received the B.S. degree in meteorology from the University of Chicago in 1944. Following the war, he continued his studies at the Massachusetts Institute of Technology and was awarded the S.M. degree in 1948 and the Sc.D. in 1951 in aeronautical engineering. Dr. Ashley joined the staff of the Massachusetts Institute of Technology as an assistant in 1946 and became an instructor in 1947. He was appointed to the faculty as an assistant professor in 1948, became associate professor in 1954, and professor in 1960, specializing in aeroelasticity and aerodynamics. As a consultant, Dr. Ashley has served a number of research organizations, industrial corporations, and government agencies, and was involved with the first manned orbital space flight. The author or co-author of more than thirty technical publications, Dr. Ashley was also co-author of *Aeroelasticity* (with R. L. Bisplinghoff and R. L. Halfman, 1955) and *Principles of Aeroelasticity* (with R. L. Bisplinghoff, 1961). Dr. Ashley is active in civic as well as professional affairs and is a fellow of the American Academy of Arts and Sciences. Dr. Ashley is also a member of the American Meteorological Society, AIAA, Phi Beta Kappa, Sigma Xi, and Tau Beta Pi.

Dr. Sheila Evans Widnall received the degrees of Bachelor and Master of Science in 1961 and the Doctor of Science degree in 1964 from the Department of Aeronautics and Astronautics at the Massachusetts Institute of Technology. In her professional experience, she has been employed for four summers by the Boeing Company of Seattle, Washington, and a summer by the Aeronautical Research Institute of Sweden. She has also been a staff member of the Division of Sponsored Research at the Massachusetts Institute of Technology and a consultant to DeHaviland Air Craft, Ltd. She has been appointed Assistant Professor at the Massachusetts Institute of Technology, working under a Ford Postdoctoral Fellowship. Her publications in the field of unsteady hydrodynamics have been co-authored by Professors Holt Ashley and Marten Landahl.

Professor Landahl received his Civilingenjor's degree from the Royal Institute of Technology (KTH), Stockholm, Sweden, in 1951; his Teknologie Licentiat in 1953; and his Doctorate in 1959. He held positions in the Swedish Air Board and at the Royal Institute of Technology from 1948 to 1954. During the summer of 1952, he was an exchange student to the Massachusetts Institute of Technology, in the Department of Aeronautical Engineering; and he returned in 1954 for two years as Division of Sponsored Research (DSR) Staff Member in the Aeroelastic Laboratory. From 1956 to 1960, he was a Senior Research Scientist at the Aeronautical Research Institute of Sweden (FFA). In 1960 he joined the faculty of the Department of Aeronautics and Astronautics as an Associate Professor. In 1963 he was promoted to the rank of full Professor. As a consultant, he has served several research organizations and industrial corporations. Dr. Landahl has published a large number of papers within the areas of aerodynamics, aeroelasticity, and hydrodynamic stability. He is also the author of the book *Unsteady Transonic Flow*.

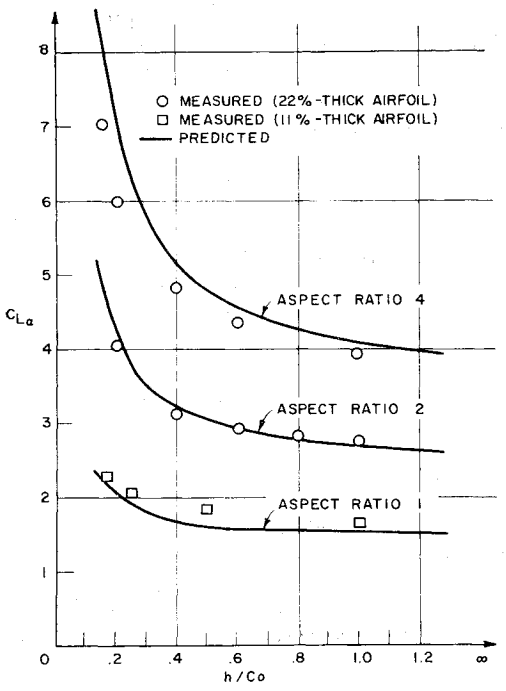

Fig. 2 Influence of height above a ground plane on steady-state lift-curve slopes of three rectangular wings in constant-density flow.

significance of the cross on the spanwise integration in Eq. (8), which is the last to be performed. K in Eq. (8) and all other acceleration-potential kernels for forward motion of three-dimensional systems at $M < 1$ have line singularities $(y - \eta)^{-2}$ or $(s - \sigma)^{-2}$.

Equation (8) is thus reduced by collocation to a set of linear, algebraic equations in the unknown complex constants a_{nm}. Solution is carried out by direct inversion or a least-squares technique. The load distribution then follows from Eq. (10), which can be integrated in various simple ways over the transformed area of S to yield generalized forces such as lift and pitching moment. The convergence of this process can be inferred by comparing the solid and dashed lift variations on Fig. 9, which were computed using 16 and 25 collocation points, respectively; this and similar studies show that

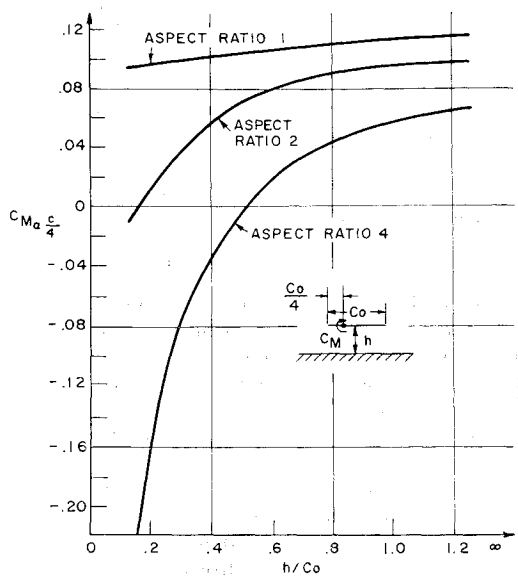

Fig. 3 Slopes of pitching moment about a quarter-chord axis for three wings in ground effect.

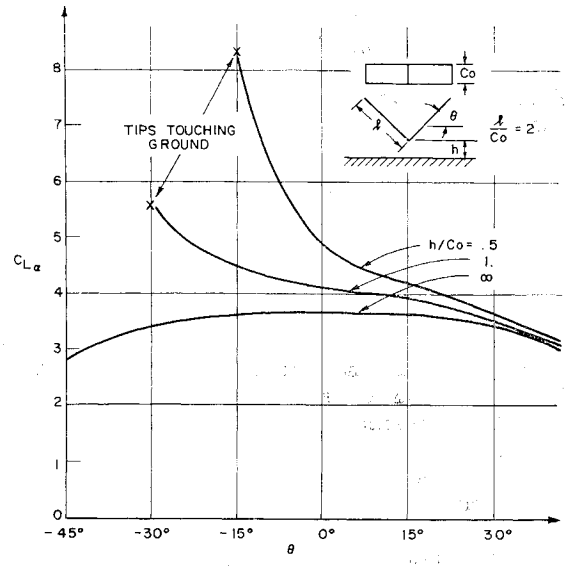

Fig. 4 Steady lift-curve slope vs dihedral angle, computed by constant-density, nonplanar lifting surface theory for a V wing at three centerline heights above ground.

16 points may usually be expected to yield generalized forces numerically correct within a percent or two.

It is observed that somewhat more refined schemes[14, 15] have been proposed for solving Eq. (8) in the planar case. They merit further examination for nonplanar surfaces.

Some Constant-Density Applications

Figures 2–12 show what can be done in various physical situations by solving Eq. (8) (or its two-dimensional counterpart) with the appropriate kernel function. Many other examples, including planar surfaces in unsteady compressible flow, may be seen in the paper by Cunningham and Woolston[16] and elsewhere.

From the recent study of steady-state ground effect in Saunders' thesis[17] are taken Figs. 2–4. Figure 2 shows the excellent accuracy that can sometimes be obtained at low in-

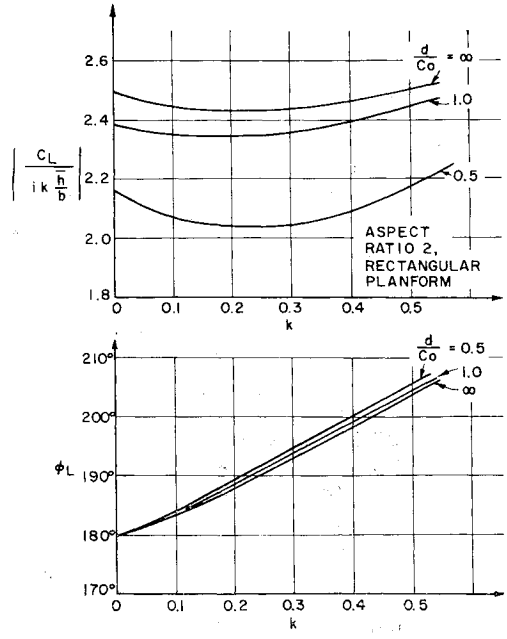

Fig. 5 Magnitude and phase of theoretical lift due to heaving oscillation, as functions of reduced frequency, for a hydrofoil running at high F and three values of depth below a free liquid surface.

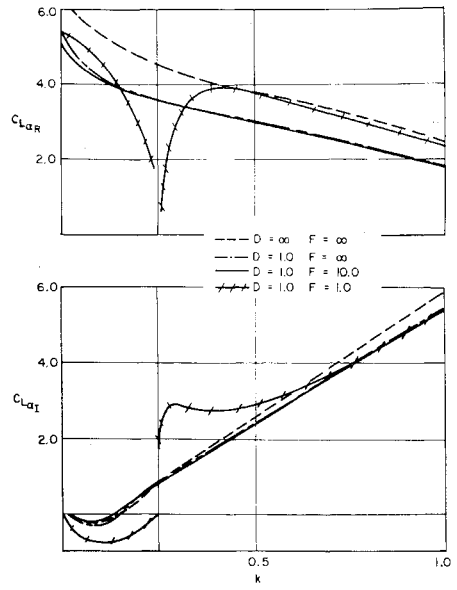

Fig. 6 Real and imaginary parts of theoretical lift-curve slope, as functions of reduced frequency, for a two-dimensional hydrofoil pitching about a quarter-chord axis. Four combinations of Froude number and depth in semichords are shown.

cidence even on thick wings. Two mutually canceling nonlinear effects, i.e., load increases due to blockage and load decrease due to reduced "effective" streamwise velocity induced by the image vortices, may be responsible for fortuitous success here. The familiar aft shift of aerodynamic center caused by approaching the ground is certainly well indicated by Fig. 3, however, and the combined action of dihedral and ground plane in Fig. 4 also agrees with what might be anticipated.

Figure 5 is one of several illustrations of free-surface influence published in Refs. 8 and 9. As discussed in the Appendix, the hydrofoil outruns its own wave train when the Froude number $F = U/(gl)^{1/2}$ is sufficiently large. The surface can then be simulated by an image performing the same motion, i.e., vertical translation (heaving) oscillation in the case of Fig. 5, as the actual foil. The ordinates are coefficient of lift, divided by the maximum angle of attack due to the (positive downward) vertical displacement $\bar{h}e^{i\omega t}$ and converted to magnitude and phase-angle form

$$\bar{C}_L = |C_L|e^{i\varphi_L} \tag{11}$$

The image is seen to cause an effective reduction of incidence without appreciable phase shift, and the influence becomes significant at depths somewhere between one and one-half chordlengths. These and similar calculations may be interpreted as suggesting that the free surface will favorably

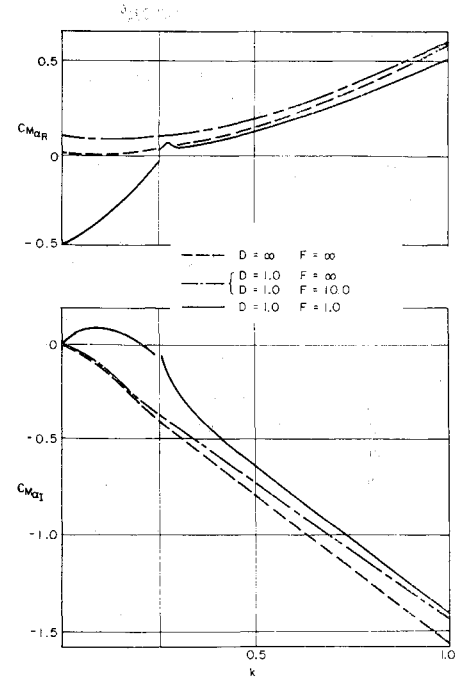

Fig. 7 Real and imaginary parts of oscillatory moment-curve slope, about the quarter-chord axis, for the hydrofoil of Fig. 6.

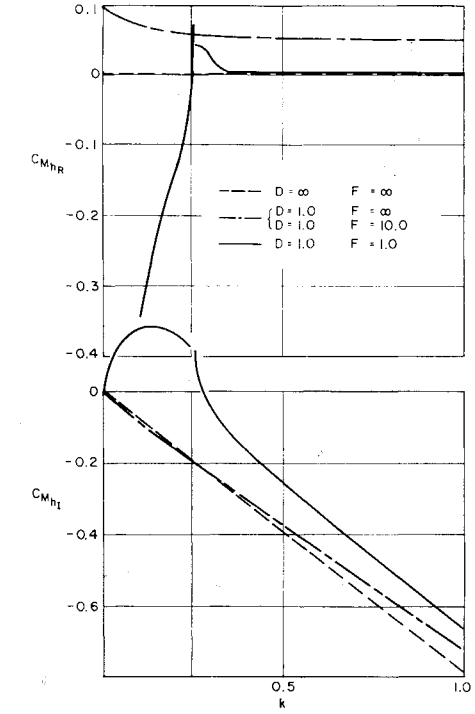

Fig. 8 Real and imaginary parts of quarter-chord moment coefficients per unit dimensionless amplitude of vertical displacement h, for the hydrofoil of Fig. 6 in heaving oscillation.

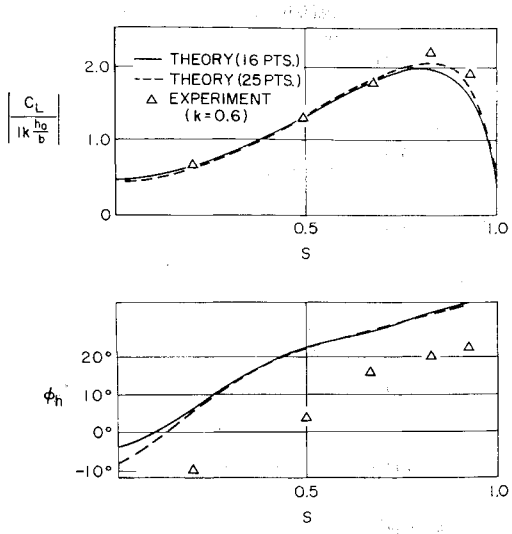

Fig. 9 Magnitude and phase of lift coefficient per unit tip-velocity amplitude for a rectangular cantilever (full-span aspect ratio 5) performing symmetrical bending oscillations in water. Lifting-surface theory, for two sizes of collocation net, is compared with the measurements of Ransleben and Abramson for $k = 0.6$.

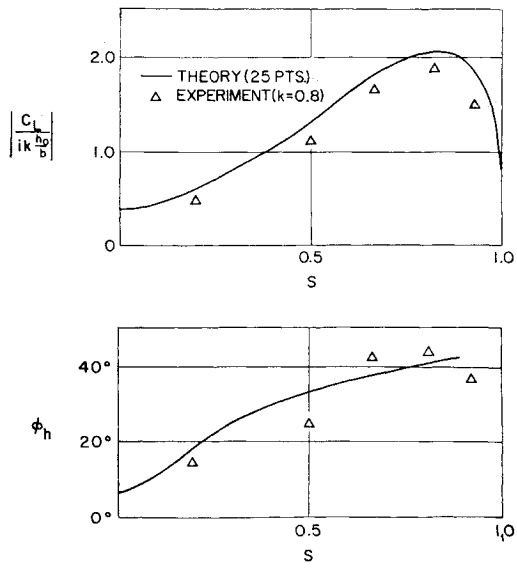

Fig. 10 Same quantities as Fig. 9, for $k = 0.8$.

affect hydroelastic stability at large F, that is, at the high speeds characteristic of hydrofoil operation.

Figures 6–8 present lift and pitching moments, due to heaving and pitching vibrations, as functions of reduced frequency for various combinations of F and dimensionless depth D. These complex quantities are available more readily in the real and imaginary decomposition, i.e.,

$$\bar{C}_L = C_{LR} + iC_{LI} \tag{12}$$

The theory here is for two-dimensional foils, including the contributions from surface waves as discussed in the fourth section of the Appendix. Perhaps the most important conclusion to be drawn from these curves is that $F = 10$ appears already high enough to permit the use of infinite-Froude-number approximations. It is reasoned that this estimate is even more valid for three-dimensional foils, where $F = 5$ may often be an adequate boundary.

Results like those in Figs. 6–8 have been compared, as $D \to \infty$, with the well-known solution for infinite depth and with a prior theory due to Crimi and Statler,[18] who worked with vortex-sheet integral equations. The former check is perfect, whereas the latter shows satisfactory qualitative agreement. Both theories yield singular loadings when $kF^2 = \frac{1}{4}$ for any finite D.

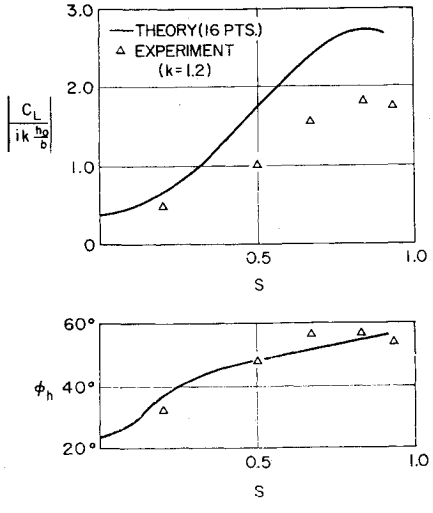

Fig. 11 Same quantities as Fig. 9, for $k = 1.2$.

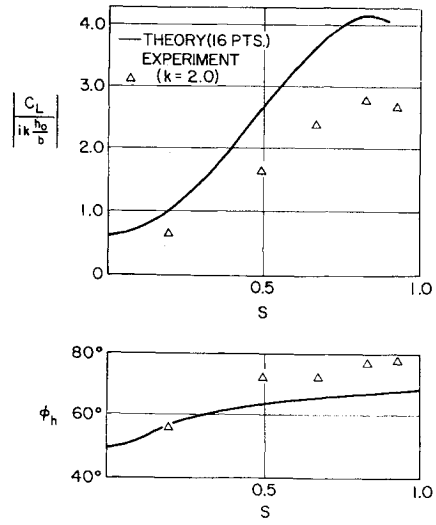

Fig. 12 Same quantities as Fig. 9, for $k = 2.0$.

Supersonic Speeds

The method of aerodynamic influence coefficients, proposed by Pines et al.[11] for simple configurations and exhaustively developed for planar supersonic wings by Zartarian and Hsu,[19] has proved very adaptable to nonplanar surfaces composed of multiple intersecting or interacting planes. Both supersonic speeds and sufficiently unsteady motions in the vicinity of $M = 1$ can be handled by this numerical mechanization of acoustic theory.

Although details can be read in two papers[10, 20] by one of the present authors, a brief résumé is in order here before applications are given. This scheme relies on the possibility at $M \geq 1$ of using source sheets, which produce symmetrical flow with respect to their own planes, in place of doublets. Communication between opposite sides of the same lifting surface must then be prevented by adding sources over properly selected "diaphragm" areas and enforcing conditions of zero pressure and normal-velocity discontinuity through these areas. Turning to Fig. 13, which presents by way of example a rectangular wingtip and its associated diaphragm, one sets out from the following expression[6] for the (dimensionless) disturbance velocity potential in the half-space $z \geq 0$:

$$\bar{\varphi}(x, y, z) = -\frac{1}{\pi} \iint_{S'} \bar{w}(\xi, \eta) \exp\left[\frac{-ikM^2(x - \xi)}{\beta^2}\right] \times \frac{\cos\{(kM/\beta^2)\,((x - 3)^2 - \beta^2[(y - \eta)^2 + z^2])^{1/2}\}}{\{(x - \xi)^2 - \beta^2[(y - \eta)^2 + z^2]\}^{1/2}}\, d\xi d\eta \tag{13}$$

In Eq. (13) $\beta = (M^2 - 1)^{1/2}$; $\bar{w}$ is proportional to the complex amplitude of source strength per unit area and here equals the vertical velocity $\bar{v}_n$ just above the surface, a known quantity on S. Integration area S' is that portion of S and the diaphragm that is intercepted by a forward Mach cone from point (x, y, z). S' is automatically covered by requiring $\xi < x$, integrating over the entire area of source sheet, and taking the real part of the result with respect to the change of sign of the quantity under the radical (as distinct from the complex unit i used to represent simple-harmonic time variation).

As in Fig. 13, wing and diaphragm are overlaid as closely as possible with elementary rectangles, having chordwise dimension units and diagonals parallel to the Mach lines. In terms of the new variables

$$x_1 = x/b_1,\ \xi_1 = \xi/b_1$$

$$y_1 = y/(b_1/\beta),\ \eta_1 = \eta_1/(b_1/\beta) z_1 = z/(b_1/\beta)$$

$$\bar{k}_1 \equiv kb_1(M^2/\beta^2)$$

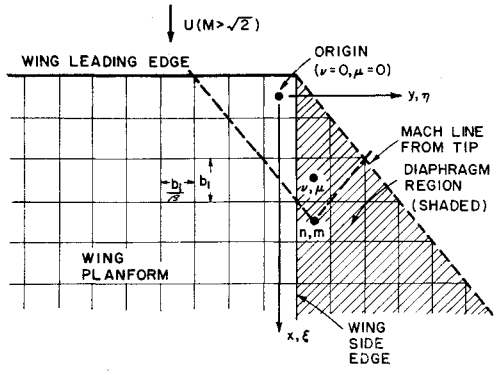

Fig. 13 Illustrating right wingtip region of a plane, rectangular wing in supersonic flow overlaid with elementary rectangular areas having diagonals parallel to the Mach lines. (ν, μ) and (n, m), respectively are pairs of integers identifying chordwise and spanwise centers of areas that "send" and "receive" signals.

Eq. (13) reads

$$\bar{\varphi}(x_1, y_1, z_1) = \frac{-b_1}{\pi\beta} \iint_{S'} \bar{w}(\xi_1, \eta_1) \times \frac{e^{-i\bar{k}_1(x_1-\xi_1)} \cos\{(\bar{k}_1/M)[(x_1-\xi_1)^2-(y_1-\eta_1)^2-z_1^2]^{1/2}\}}{[(x_1-\xi_1)^2-(y_1-\eta_1)^2-z_1^2]^{1/2}} \, d\xi_1 d\eta_1 \tag{14}$$

Finally, it is assumed (as will be true in the limit $b_1 \to 0$) that $\bar{w}$ is constant over each rectangle and equal to the value $\bar{w}_{\nu,\mu}$ at the center. After some manipulation, one is led to the algebraic result

$$\bar{\varphi}(x_1, y_1, z_1) = \frac{b_1}{\beta} \sum_{\nu,\mu} \bar{w}_{\nu,\mu} \Phi_{\bar{\nu},\bar{\mu},z_1} \tag{15}$$

where the sum extends over all elements wholly or partially intercepted by S'. The aerodynamic influence coefficient $\Phi_{\nu,\bar{\mu},z_1}$ depends only on the relative positions

$$\bar{\nu} \equiv (x_1 - \nu)$$

$$\bar{\mu} \equiv (y_1 - \mu), z_1$$

between the "sending" area and "receiving" point. It can be written

$$\Phi_{\bar{\nu},\bar{\mu},z} = -\frac{1}{\pi} \int_{\bar{\nu}-1/2}^{\bar{\nu}+1/2} \int_{\bar{\mu}-1/2}^{\bar{\mu}+1/2} e^{-i\bar{k}_1\bar{\xi}_1} \times \frac{\cos[(\bar{k}_1/M)(\bar{\xi}_1^2-\bar{\eta}_1^2-z_1^2)^{1/2}]}{(\bar{\xi}_1^2-\bar{\eta}_1^2-z_1^2)^{1/2}} \, d\bar{\xi}_1 d\bar{\eta}_1 \tag{16}$$

where $\bar{\xi}_1 \equiv (x_1 - \xi_1)$, $\bar{\eta} \equiv (y_1 - \eta_1)$, and the "real part" is understood to be taken with respect to the quantity under the radical. It has been shown[19, 20] how $\Phi_{\bar{\nu}_1,\bar{\mu},z_1}$ can be computed by a single numerical integration of an infinite series of Bessel functions J_{2n} with excellent convergence properties.

In the same way, the dimensionless velocity components at a field point are expressible as

$$\bar{v}(x_1, y_1, z_1) = \sum_{\nu,\mu} \bar{w}_{\nu,\mu} V_{\bar{\nu},\bar{\mu},z_1} \tag{17}$$

$$\bar{w}(x_1, y_1, z_1) = \sum_{\nu,\mu} \bar{w}_{\nu,\mu} W_{\bar{\nu},\bar{\mu},z_1} \tag{18}$$

References 19 contain numerous illustrations, for planar wings in steady or oscillatory motion, of the computation of velocity potential and airload distributions by means of Eq. (15). The continuity requirement at each diaphragm element supplies a condition which fixes the value of $\bar{w}_{\nu,\mu}$ at its center.

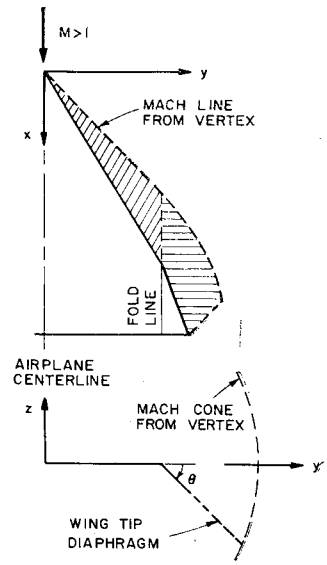

Fig. 14 Top and rear elevations of a triangular wing in supersonic flow with wingtip folded downward. Shown shaded is a suitable diaphragm area for isolating the upper and lower surfaces.

For the simple geometries where they are available, exact linearized solutions provide good confirmation of the numerical results, provided certain simple rules are followed. The questions of leading-edge singularities, upwash singularities, and wake diaphragms have been thoroughly studied.[19]

References 10 and 20 discuss the extension to intersecting or interfering surfaces, which is complicated by the fact that source-sheet strengths no longer fix the local normal velocities. Equations (15, 17, and 18) must be used in combination to produce coupled algebraic relations that assure flow tangency at the center of each lifting-surface area element and continuity through each diaphragm element. Fortunately, as with planar wings, the computation can be so ordered that no system of simultaneous equations ever needs to be inverted. The number of steps is nevertheless enormous, so that a computer of the size of IBM 7090 is essential.

Routines for load determination on vibrating nonplanar surfaces are now in operation. Only steady-flow examples, however, are available for presentation here. Figure 14 pictures a configuration on which considerable work has been done, showing a suitable diaphragm arrangement for isolating the upper and lower surfaces. Figure 15 compares lift-curve slopes for this wing, obtained by Johnson and Andrew[12] with a modified version of the Ref. 20 procedure, against wind-tunnel data[21] at three angles of wingtip rotation. Supersonic Mach numbers between 1.2 and 3.0 are covered, as well as subsonic predictions from Eqs. (8) and (A3) with Prandtl-

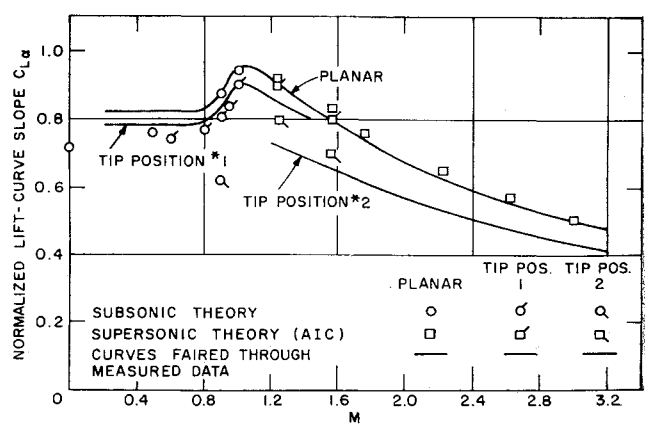

Fig. 15 Steady lift-curve slopes, plotted vs Mach number and normalized to the planar-wing value at $M = 1$, for three tip positions on the wing of Fig. 14. (Courtesy of North American Aviation, Inc.)

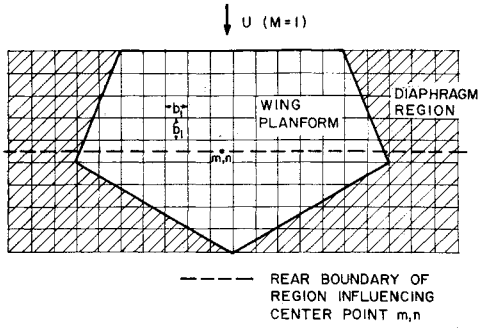

Fig. 16 Pattern of square area elements suitable for approximating a wing-diaphragm combination in sonic flight.

Glauert scaling. Although the quantitative agreement is not perfect, linear theory does seem able to estimate the change in loading due to tip droop on this very surface, and aerodynamic-center measurements confirm this conclusion.

Transonic Speeds

Landahl,[22] Miles,[23] and others have noted that, although lifting surfaces in steady flight near $M = 1$ cannot be given a fully linear treatment, the oscillatory case is governed by the differential equation

$$\bar{\varphi}_{yy} + \bar{\varphi}_{zz} - 2ikM^2\bar{\varphi}_x + k^2M^2\bar{\varphi} = 0 \qquad (19)$$

whenever $k \gg |1 - M|$ and local Mach-number variations near the surface due to thickness, etc., are not too great. Equation (19) also implies a similarity law,[22] by which flow at any M in the transonic range can be referred to a sonic counterpart:

$$\bar{\varphi}(x, y, z;\ M, k) = (1/M)\bar{\varphi}(x, My, Mz;\ M = 1, k) \qquad (20)$$

There is a sonic source sheet solution of Eq. (19), corresponding to Eq. (13) or (14), which can form the basis for an influence-coefficient procedure. The scheme proposed by one of the authors is presented in Fig. 16, where the lifting area and diaphragm are shown subdivided into square elements of (dimensionless) side b_1. With Mach lines parallel to the y axis, the diaphragm would extend laterally to infinity. Hence the source strengths beyond a certain distance away from each tip must be arbitrarily equated to zero. The exact solution[22] for a quarter-infinite wing provides good justification for this step, although the diaphragm may sometimes have to be extended out several chordlengths.

In terms of coordinates referred to b_1, the source-sheet potential reads

$$\bar{\varphi}(x_1, y_1, z_1) = \frac{-b_1}{\pi}\int_{x_{1L}}^{x_1}\int_{-\infty}^{\infty} \bar{w}(\xi_1, \eta) \times \frac{\exp\{-(ik/2)|x_1 - \xi_1 + [(y_1 - \eta_1)^2 + z_1^2]/(x_1 - \xi_1)|\}}{[x_1 - \xi_1]}\, d\eta_1 d\xi_1 \qquad (21)$$

Here $k_1 \equiv kb_1$. Formulas like (17, 18, and 15) (with $\beta = 1$) may be carried over directly, the summations encompassing all area elements ahead of the "receiving" point. Individual aerodynamic influence coefficients can be expressed as single chordwise integrals containing Fresnel functions. They are substantially easier to compute than their supersonic counterparts, and loading calculation on both planar and nonplanar wings appears correspondingly less arduous, although some matrix inversions are required when treating the diaphragm.

The first applications of the foregoing scheme, as yet unpublished, have been made by Weatherill at the Boeing Company. Figures 17 and 18 graph some of his preliminary results. The comparison between the exact and numerical potential distributions due to heaving oscillation at $k_1 = 0.05$ (Fig. 17) is seen to be extraordinarily accurate. The slight deviations beyond about 14 elements chordwise are attributed to the arbitrary termination of the source sheet at 80 elements to either side of the reference section; the finite span of the influence-coefficient representation is beginning to make itself felt.

Figure 18 plots, vs reduced frequency based on midspan semichord, the magnitude of lift due to heaving of planar delta surfaces. The ordinate is made dimensionless in such a way[22] that all curves should coincide if the calculations and the similarity law, Eq. (20), were both exact. A network of area elements was used in the numerical prediction which would have been more than adequate at higher supersonic M. The significant differences between Landahl's results and their aerodynamic-influence-coefficient counterparts, both at sonic and low supersonic speeds, indicate that further study is needed to establish the required fineness of these networks in the transonic range.

Limitations of Linearized Theory

The considerations of the next two sections are more speculative in the sense that some refinements are proposed which have not yet been demonstrated in practice, although their feasibility is unquestioned on modern digital computers. Furthermore, no attention is devoted to lifting surface

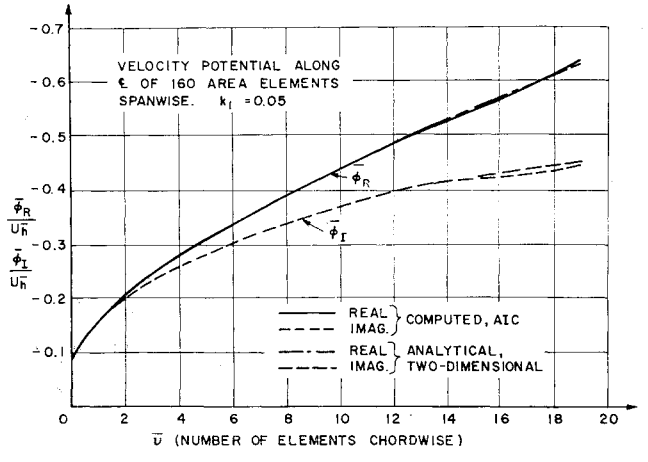

Fig. 17 Real and imaginary parts of theoretical dimensional velocity potential, plotted vs chordwise distance for a heaving wing in sonic flight. Numerically computed result is based on aerodynamic influence coefficients with 80 area elements on either side of the station. (Courtesy of The Boeing Co.)

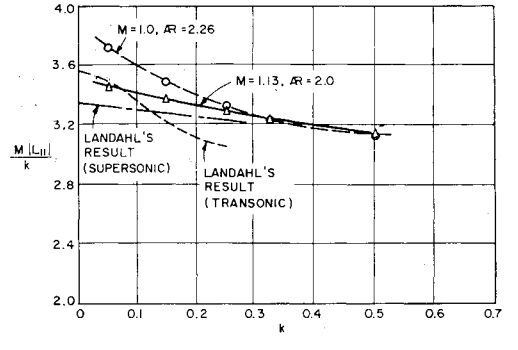

Fig. 18 Amplitude of dimensionless theoretical lift due to heaving oscillation for two delta wings at different transonic Mach numbers. Exact solutions vs k are compared with numerical estimates (triangles and circles) by and supersonic aerodynamic influence coefficients. (Courtesy of The Boeing Co.)

problems connected with flow separations, such as high incidence, spoilers, and blunt trailing edges. The vital importance of these phenomena is recognized, and the reader may be referred to the appropriate chapters of recent books by Thwaites[24] and Woods[25] for some imaginative theoretical contributions. The intent here, however, is to examine how the numerical formulation of unseparated, ideal flow can be improved and generalized, with special regard to arbitrary interacting systems and unsteady motion. A primary objective is tools for final design and analysis of thin, high-speed configurations, i.e., tools which can serve as a potent complement to the costly experimental approach.

Failure of the Kutta-Joukowsky Hypothesis at High Reduced Frequency

The first measurements of oscillatory airloads that were carried up to k's of unity were made on two-dimensional airfoils by Greidanus, van de Vooren, and Bergh.[26] Recently, Ransleben and Abramson[27] have published high-k data taken in water on a rectangular wing performing elastic flexural and torsional vibrations. Measured force and moment amplitudes tend to fall below the linearized theoretical values as k increases through about $\frac{1}{2}$ in the two-dimensional case and 1 on the wing of aspect ratio 5. Both sets of authors suggest a lag in fulfillment of the smooth flow-off condition at the trailing edge and/or displacements of the wake vortex sheet from a plane as possible explanations. Unfortunately, both experimental procedures varied k by changing the velocity at fixed frequency, so that independent examination of the influences of k and Reynolds number was impossible. Also, the three-dimensional amplitudes[27] may be somewhat below their true experimental values at high k because of interference with the dynamometers by gap-sealing material. Nevertheless, the disagreement certainly deserves careful theoretical analysis because of its implications for the flutter problem, and linearized theory of the type described above offers one avenue.

As a test of the best classical theory against the three-dimensional data, Figs. 9–12 plot solutions of Eq. (8) in amplitude-phase form vs the Ref. 27 results for bending vibration. Spanwise lift distributions are presented for four, successively larger values of k. All phase angles are believed to compare within the probable experimental error, but the falling off of measured amplitudes between $k = 0.8$ and 1.2 is quite evident.

A thorough analysis of what happens to the Kutta-Joukowsky hypothesis with increasing reduced frequency would require imaginative developments in unsteady boundary-layer theory for wings with varying circulation. But a semi-empirical test of the suggested lag in flow-off from the trailing edge is not so difficult. A lead can be taken from George's two-dimensional theory.[28] One simply relaxes the condition by adding a trailing-edge singularity of adjustable amplitude to the series of Eq. (10). One finds by trial and error whether this amplitude can be set so as to match the data of Refs. 26 and 27. Such an investigation is now in progress. If successful, it would provide strong impetus for more sophisticated work on flow near trailing edges at high frequency.

Distortion of the Wake

As is well known, the loading of a thin subsonic wing is influenced only to order α^3 by displacements of the wake from the projected wing plane. This effect is much larger, however, in certain other situations. When interference of the wake on an aft empennage is estimated, for instance, appreciable rolling up may have occurred. There are also problems where the lifting surface's path through the fluid is not rectilinear, and here again the computer proves its usefulness whereas exact solutions fail.

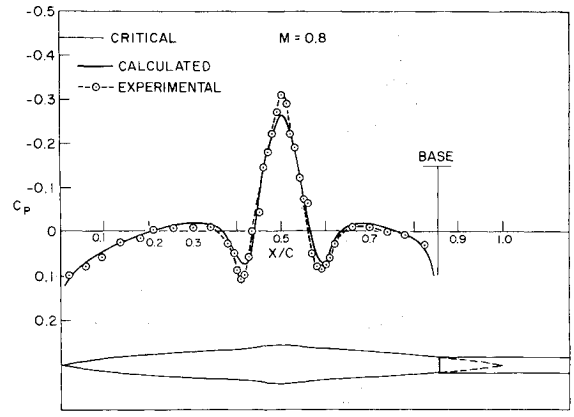

Fig. 19 Comparison of experimental and calculated pressure coefficients on the bumpy body.

An example of the latter sort is Miller's numerical theory[29,30] of unsteady airloads on a helicopter rotor in forward flight. By partially introducing nonlinearity, i.e., causing each wake vortex element to move with the instantaneous inflow velocity near the trailing edge at the moment the element was shed, he obtained improved agreement with experiment and thus helped to clarify one of the severest design problems on rotary-wing aircraft.

As a second illustration, one can cite unpublished unsteady-flow calculations by North American Aviation, Inc. By assuming the wake of a horizontal canard surface to be fully rolled up as it passed the main wing and to follow the path of the steady wake observed in the wind tunnel, better estimates of canard-wing interaction were achieved than could be obtained with a planar wake.

Nonlinearity Associated with Wing Shape and Location

Perhaps the most comprehensive limitations of classical theory, as adapted both to steady and time-dependent loading, came about because of the second- and higher-order effects of thickness distribution, mean angle of attack, camber, and nearness to a flow boundary. All of these have been thoroughly analyzed for mathematically simple, planar configurations in steady subsonic and supersonic flight; extended review of the literature is impractical here. Thickness can fairly be described as the most interesting of these effects. Its contribution to Δp is of second order in the small parameter ϵ, and one useful fact is that this influence can be inserted into linear relationships between generalized aerodynamic forces and the motion coordinates that produce them.

For constant-density fluid and for the transonic-supersonic regime, the next section discusses a few ways in which numerical theories may be improved beyond first-order linearity.

Some Contributions to Nonlinear Unsteady Wing Theory

Constant-Density Flow

An obvious but nontrivial remark is that these theories should be vastly more tractable than compressible-flow problems because of the linear field differential equation. This has turned out to be the case, particularly in two dimensions where the complex variable may be invoked, and recent successes with nonlinear methods for steady and acyclic phenomena offer encouragement.

For ten years A. M. O. Smith and his collaborators[31–33] have refined their techniques, based on the integral equation of a source sheet over the body surface, for computing the instantaneous liquid motion due to arbitrary displacements of an arbitrary three-dimensional object. Figure 19 by Hess[32] is

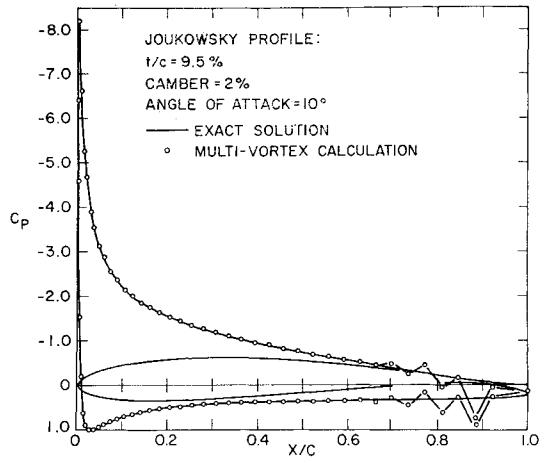

Fig. 20 Theoretical pressure coefficients on a profile in constant-density flow, calculated by exact and discrete-vortex theories.

typical of the sort of experimental comparisons their routines can achieve, even on shapes that are intentionally distorted to generate large gradients in the flow. This example also brings in compressibility, in a quasi-linear fashion, by elongating the body coordinates according to Goethert's version of the Prandtl-Glauert rule so as to get an effective Mach number of 0.8.

It would seem desirable that these techniques be extended to loading problems with circulation and wakes, but more recent experience confirms that vortex or potential-discontinuity sheets without sources are likely to prove more efficient. Characteristic of current developments in the steady-flow area by the American aircraft industry are the reports by Rubbert[34, 35] and Davenport,[36] from which Figs. 20–22 are reproduced. Figures 20 and 21 show what can be done in two dimensions by locating a large number of concentrated vortex lines on the profile surface and satisfying the flow-tangency boundary conditions through collocation at intermediate stations. The oscillatory deviation of local pressure coefficients from the exact solution, near the trailing edge of the airfoil in Fig. 20, is intentionally displayed because Rubbert has found that it can be eliminated. This is done by a combination of more careful attention to boundary conditions in the troublesome region and replacement of the concentrated vortices with a large number of short lengths of planar, distributed vortex sheets.

Ground effect, as computed by the image method, is displayed for a two-dimensional line airfoil with flap in Fig. 21. The forementioned falling off of Δp due to the nonlinear influence of the image vortices is clearly evident here. Figure 22 typifies results of a three-dimensional generalization of the vortex method, in which quadrilateral patches of spanwise and chordwise vorticity are applied over the lifting area, each having its own arbitrarily oriented trailing horseshoe. Again, the wing is preserved as a stream surface by suitable collocation. This approach has been successfully used on the nonlinear effects of control surfaces, jet flaps, and separated regions.

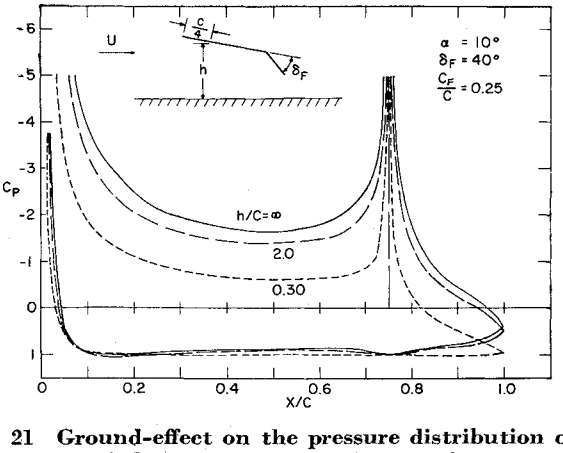

Fig. 21 Ground-effect on the pressure distribution of a flat-plate airfoil with flap, as estimated for constant-density flow by nonlinear numerical vortex-sheet theory.

Major steps toward unsteady, nonlinear lifting-surface theory for incompressible flow are the contributions of Kussner and von Gorup,[37] and of van de Vooren and van de Vel.[38] The latter authors improve on the results of Ref. 37 by satisfying the boundary conditions for heaving and pitching vibration always at the profile surface rather than at its mean position.

Turning to three-dimensional unsteady loading of general shapes, for which only a numerical formulation is conceivable, one can speculate on how the efficiency of vortex-sheet methods[38] may be carried over to the wing with a time-dependent wake. For instance, the motion might be regarded as a transient, starting at $\tau = 0$ and preceding such that the known lifting-surface position is given by

$$S(x, y, z, \tau) = 0 \tag{22}$$

$\tau = Ut/l$ being dimensionless time. A zero-thickness wake surface

$$W(x, y, z, \tau) = 0 \tag{23}$$

begins to emerge from the trailing edge.

The boundary-value problem at successive instants of time can be solved with a vortex sheet over $S + W$, starting from the information that there is no wake at $\tau = 0$. Thus, for a lifting surface without thickness in the presence of a uniform stream parallel to x, the perturbation potential φ has a discontinuity that must satisfy

$$\frac{1}{4\pi} \oint\!\!\!\!\!\!\int_{S+W} \Delta\varphi \left[\frac{\partial^2}{\partial n \partial n_1}\left(\frac{1}{r}\right)\right] dS = -\frac{\partial n}{\partial \tau} - \mathbf{i}\cdot\mathbf{n} \tag{24}$$

on $S = 0$. Here n is the "upward" normal direction from S, $\mathbf{i}$ and $\mathbf{n}$ are unit vectors, and $r \equiv [(x - \xi)^2 + (y - \eta)^2 + (z - \zeta)^2]^{1/2}$. The instantaneous mean value of φ on S or W is

$$\varphi_{\text{mean}} = \frac{1}{4\pi} \oint\!\!\!\!\!\!\int_{S+W} \Delta\varphi \left[\frac{\partial}{\partial n}\left(\frac{1}{r}\right)\right] dS \tag{25}$$

The position and vortex-sheet strength of the wake after any short time step can be found from the normal and mean-tangential velocity components at the trailing edge and at $W = 0$ for the beginning of this step. The requirement of no pressure discontinuity through the wake is met only when

$$\frac{D}{D\tau}\Delta\varphi = \left[\frac{\partial \Delta\varphi}{\partial \tau} + \left(\mathbf{i} + \text{grad}\varphi_{\text{mean}} + \mathbf{n}\frac{\partial \varphi}{\partial n}\right)\cdot \text{grad}\Delta\varphi\right] = 0 \tag{26}$$

on $W = 0$.

Although the foregoing procedure would seem most promising for the calculation of indicial loading, there is no theoretical objection to using it for simple harmonic motion from a transient start. Whether computational divergence, difficulty with the wake edges curling up, and the like would interfere with the approach to steady-state oscillation remains to be seen.

Transonic and Supersonic Flow

Evidently one must first seek improved load-estimation methods of compressible fluid by way of second-order potential theory. The key physical and mathematical ideas are set forth by Lighthill,[39] and a suggestive application with

special significance for steady transonic flow is the "local linearization" concept of Spreiter and Alksne.[40] Several second-order supersonic solutions have also been published, particular mention being made of the uniformly-valid results by Clarke and collaborators.[41]

The focus in Ref. 40 is on symmetrical, two-dimensional profiles; the range $M > 1$ is treated as a special case that is shown equivalent to ordinary shock-expansion. One suspects that local linearization is adaptable both to lifting problems and to three dimensions, however, and this seems to be the real import of Covert's work[42] on steady supersonic flow. Covert demonstrates how second-order effects of thickness in the near field can be properly accounted for if the disturbance potential of the lifting flow satisfies the differential equation

$$(M_p^2 - 1)\varphi_{xx} - \varphi_{yy} - \varphi_{zz} + \delta\varphi_x = 0 \qquad (27)$$

Here M_p is the local surface Mach number due to the thickness distribution, and δ is usually a very small parameter.

φ can be built up of source-like solutions depending on M_p rather than freestream M. A correction is thus made for variations in sound speed and local convection, but third-order shock effects are ignored. There is no evident reason why Covert's scheme cannot be applied to nonplanar wings or interacting systems. Experimental data on the thickness flow could readily be incorporated.

Local linearization should also facilitate the analysis of second-order oscillatory loading. There exists a particularly interesting possibility for flight Mach numbers near unity, already given preliminary study by one of the authors,[43, 44] which promises straightforward generalization to $M > 1$. References 43 and 44 commence by applying the Kaplun-Lagerstrom expansion[7] to a point source oscillating in a nonuniform main stream. To second order in small disturbances, the differential equation reads

$$\partial/\partial x[(a_p^2 - u_p^2)\bar{\varphi}_x] - 2iku_p\bar{\varphi}_x + k^2\bar{\varphi} + a_p^2[\bar{\varphi}_{yy} + \bar{\varphi}_{zz}] = 0 \qquad (28)$$

where $u_p(x, y, z)$ and $a_p(x, y, z)$ are, respectively, local values of the x velocity and the speed of sound in the stream.

By specializing the u_p and a_p that are functions of x only, it proves possible[44] to write down fairly simple potentials for the near and far fields of the source, as well as uniformly-valid representations to first order in a small parameter dependent on local deviations of the Mach number from unity. Two- and three-dimensional source solutions are given, both for subsonic and supersonic Mach number at the source's position.

The influence of thickness on oscillatory pressure distribution can be incorporated by replacing the lifting surface with sheets of these sources, or of doublets constructed by normal differentiation. Local properties u_p and a_p would be taken as the values at the surface due to the symmetrical thickness flow, their variations in the y and z directions being neglected (cf. Spreiter and Alksne[40]). An integral equation for the source or doublet strengths can be derived by applying the condition of prescribed normal velocity component.

If the trailing-edge Mach number is locally subsonic, special care will have to be taken in this neighborhood, especially when choosing a form for the upwash in the wake just behind this edge. It can be shown that the trailing-edge effect, when an aerodynamic-influence-coefficient type of scheme is employed, may make surface-pressure contributions of order unity for a distance $(1 - M_{TE})lk$ forward. Hence the same kind of investigation will be necessary on this and several related problems as has been done for side- and leading-edge singularities in linearized supersonic flow (Zartarian and Hsu[19]).

Finally, it is remarked that the Ref. 44 sources may open up the road to a completely nonlinear unsteady solution, at least when the fluid remains homentropic. If the source sheet is regarded as the origin of all flow perturbations, then the local stream at any one source can be treated as the sum of contributions from all the others. By digitizing the source sheet, a collocation or iteration process might be devised to solve simultaneously for the entire flow due to thickness and oscillatory incidence.

Conclusions

Regarding the prediction of loadings on three-dimensional wings and interacting systems by means of linearized aerodynamic theory, it can be concluded that a pattern of self-consistent numerical approaches is emerging. Questionably consistent approximations are being replaced, as final design tools, by the systematic superposition of appropriate singularities which, in the limit, could produce an exact solution. The enabling factor is the high-speed digital computer. The linearized formulation is suggested to be a fait accompli, and numerous examples have been shown or cited in evidence.

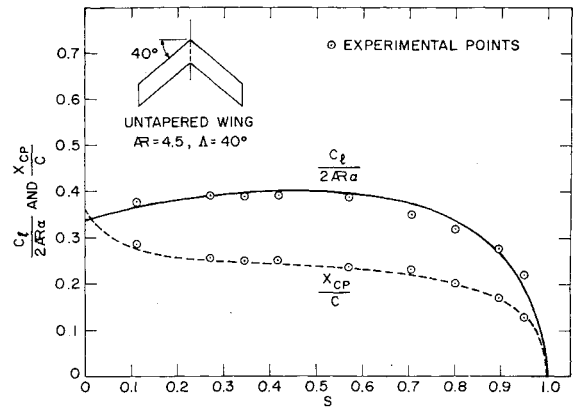

Fig. 22 Spanwise distributions of dimensionless lift and center-of-pressure location (behind leading edge), as estimated for a swept-back wing by three-dimensional vortex-sheet theory.

Ways for overcoming the inherent limitations of linearization remain largely in the form of untried proposals, except for rather special configurations in steady flow. Corrections have been suggested here for partial failure of the Kutta-Joukowsky hypothesis, for nonplanar wake effects, and for nonlinear influences such as that of wing thickness. Although one may be optimistic in the light of computer potentialities, a large amount of practical realization remains to be accomplished.

Appendix: Some Typical Subsonic Problems and Corresponding Kernel Functions

Single Nonplanar Lifting Surface

By combining Eqs. (6) and (7), one determines that the kernel function at $M < 1$ for the wing in Fig. 1 without a free surface can be formally written

$$K[(x - \xi), (y - \eta), z_0(y), z_0(\eta); M, k] = \lim_{z \to z_0(y)} \left\{ e^{-ik(x-\xi)} \frac{\partial^2}{\partial n \partial n_1} \times \int_{-\infty}^{x-\xi} \frac{\exp ik[(\lambda_1 - MR_1)/(1 - M^2)]}{R_1} d\lambda_1 \right\} \qquad (A1)$$

where

$$R \equiv \{\lambda^2 + (1 - M^2)[(y - \eta)^2 + (z - z_0(\eta))^2]\}^{1/2}$$

From the figure, one finds that

$$\frac{\partial}{\partial n} = \cos[\theta(y)]\frac{\partial}{\partial z} - \sin[\theta(y)]\frac{\partial}{\partial y}$$

$$\frac{\partial}{\partial n_1} = \cos[\theta(\eta)]\frac{\partial}{\partial z_0(\eta)} - \sin[\theta(\eta)]\frac{\partial}{\partial \eta}$$

$$= -\left\{\cos[\theta(\eta)]\frac{\partial}{\partial z} - \sin[\theta(\eta)]\frac{\partial}{\partial y}\right\}$$

the last equality resulting from the dependence in Eq. (A1) on $(y - \eta)$ and $[z - z_0(\eta)]$ only. After considerable manipulation, the following working form of K is derived for $M = 0$:

$$K_0 = \sin[\theta(y) + \theta(\eta)]\frac{y_0 z_{00}}{r_1^4}\left\{\frac{x_0[3r_1^2 + 2x_0^2]}{r_0^3} - i\frac{kx_0^2}{r_0} - ike^{-ikx_0}\int_0^{x_0}\frac{\lambda e^{ik\lambda}d\lambda}{(\lambda^2 + r_1^2)^{1/2}} - k^2e^{-ikx_0}\int_0^{x^0}\frac{\lambda^2 e^{ik\lambda}d\lambda}{(\lambda^2 + r_1^2)^{1/2}} + k_1^2e^{-ikx_0}\left[K_2(k_1) - \frac{\pi i}{2}[I_2(k_1) - L_2(k_1)] + \frac{ik_1}{3} - \frac{i}{k_1}\right]\right\} -$$

$$\cos\theta(y)\cos\theta(\eta)\frac{1}{r_1^2}\left\{\frac{y_0^2}{r_1^2}\left[-\frac{x_0}{r_0} + ike^{-ikx_0}\int_0^{x_0}\frac{\lambda e^{ik\lambda}d\lambda}{(\lambda^2 + r_1^2)^{1/2}}\right] + \frac{z_{00}^2}{r_1^2}\left[\frac{x_0[2r_1^2 + x_0^2]}{r_0^3} - i\frac{kx_0^2}{r_0} - k^2e^{-ikx_0}\int_0^{x_0}\frac{\lambda^2 e^{ik\lambda}d\lambda}{(\lambda^2 + r_1^2)^{1/2}}\right] - k_1e^{-ikx_0}\left[K_1(k_1) + \frac{\pi i}{2}[I_1(k_1) - L_1(k_1)] - i\right] + k_1^2\frac{z_{00}^2}{r_1^2}e^{-ikx_0}\left[K_2(k_1) - \frac{\pi i}{2}[I_2(k_1) - L_2(k_1)] + \frac{ik_1}{3} - \frac{i}{k_1}\right]\right\} -$$

$$\sin\theta(y)\sin\theta(\eta)\frac{1}{r_1^2}\left\{\frac{z_{00}^2}{r_1^2}\left[-\frac{x_0}{r_0} + ike^{-ikx_0}\int_0^{x_0}\frac{\lambda e^{ik\lambda}d\lambda}{(\lambda^2 + r_1^2)^{1/2}}\right] + \frac{y_0^2}{r_1^2}\left[\frac{x_0[2r_1^2 + x_0^2]}{r_0^3} - i\frac{kx_0^2}{r_0} - k^2e^{-ikx_0}\int_0^{x_0}\frac{\lambda^2 e_{ik\lambda}d\lambda}{(\lambda^2 + r_1^2)^{1/2}}\right] - k_1e^{-ikx_0}\left[K_1(k_1) + \frac{\pi i}{2}[I_1(k_1) - L_1(k_1)] - i\right] + k_1^2\frac{y_0^2}{r_1^2}e^{-ikx_0}\times\left[K_2(k_1) - \frac{\pi i}{2}[I_2(k_1) - L_2(k_1)] + \frac{ik_1}{3} - \frac{i}{k_1}\right]\right\} \quad \text{(A2)}$$

Here I_1, K_1, and L_1 are modified Bessel and Lommel functions in standard notation. The auxiliary symbols are as follows:

$$x_0 \equiv x - \xi \qquad y_0 \equiv y - \eta$$

$$z_{00} \equiv z_0(y) - z_0(\eta) \qquad r_1 \equiv (y_0^2 + z_{00}^2)^{1/2}$$

$$r_0 \equiv (x_0^2 + y_0^2 + z_{00}^2)^{1/2} \qquad k_1 \equiv kr_1$$

The corresponding kernel function K for nonzero Mach number contains the same singularities, the same special functions, and the same sort of integrals to be evaluated numerically over finite ranges as does K_0. It is not reproduced here, because to write it requires space roughly three times that consumed by Eq. (A2).

Steady Flow

The steady-flow counterpart of Eq. (A1) is derived by taking the limit of Eq. (A2) as $\omega \to 0$. Only the case $M = 0$ need be presented, because subsonic compressible flow can be handled by the Prandtl-Glauert rule:

$$y_0^2(K_0)_{\omega=0} =$$

$$\sin[\theta(y) + \theta(\eta)]\frac{y_0^3 z_{00}}{r_1^4}\left[2 + \frac{x_0(3r_1^2 + 2x_0^2)}{r_0^3}\right] - \cos\theta(y)\cos\theta(\eta)\frac{y_0^2 z_{00}^2}{r_1^4}\left[1 + \frac{x_0(2r_1^2 + x_0^2)}{r_0^3} - \frac{y_0^2}{z_{00}^2}\left(1 + \frac{x_0}{r_0}\right)\right] - \sin\theta(y)\sin\theta(\eta)\frac{y_0^4}{r_1^4}\left[1 + \frac{x_0(2r_1^2 + x_0^2)}{r_0^3} - \frac{z_{00}^2}{y_0^2}\left(1 + \frac{x_0}{r_0}\right)\right] \quad \text{(A3)}$$

Ground Plane or Free Liquid Surface at High Froude Number

By the familiar image principle, a ground plane such as can be imagined by inverting Fig. 1 is accounted for by adding to the field a second wing, which is loaded in a sense symmetrical to the original wing. When a hydrofoil moves at high Froude number F under a free liquid surface, it outruns the resulting wave pattern. With $F \gg 1$, it is easily shown that the boundary condition of constant pressure at $z = D$ reduces to $\varphi = 0$, which is enforced by loading the image wing in an antisymmetrical sense, that is, by having the vertical components of $\Delta\rho$ parallel in Fig. 1 whereas the horizontal components are antiparallel.

In both these cases, the added sheet of ψ doublets simply causes an additive correction to K in Eq. (8). For example, consider a planar foil parallel to the free surface at $z = D$ with $M = 0$. Area S then lies on the x-y plane. One constructs the required kernel by first setting $\theta(y) = \theta(\eta) = 0$ and $z_{00} = 0$ in Eq. (A2); to the result is added the same K_0 with $\theta(y) = \theta(\eta) = 0$ and $z_{00} = -2D$.

Free Surface Effect in Two Dimensions of Arbitrary Froude Number

This case was first treated by the efficient ψ doublet approach in Ref. 8. Naturally, only a single integral equation is involved:

$$\bar{v}_n(x) = \oint_{x_L}^{x^T}\frac{\Delta p(\xi)}{\rho_\infty U^2}K_{2D}d\xi \quad \text{(A4)}$$

The kernel function reads[8, 9]

$$K_{2D}(x - \xi;\ k, D, F) = \frac{-1}{2\pi x_0} + \frac{ike^{-ikx_0}}{2\pi}\left[Ei(ikx_0) + \frac{\pi i}{2}\left(1 + \frac{|x_0|}{x_0}\right)\right] - \frac{x_0}{2\pi(x_0^2 + 4D^2)} - \frac{ik}{4\pi}e^{-q_0}\left[Ei(q_0) + \pi i\left(1 + \frac{|x_0|}{x_0}\right)\right] + \frac{ia_1}{4\pi}e^{-q_1}\left[Ei(q_1) + \pi i\left(1 + \frac{|x_0|}{x_0}\right)\right] + \frac{ia_2}{4\pi}e^{-q_2}\left[Ei(q_2) + \pi i\left(1 + \frac{|x_0|}{x_0}\right)\right] - \frac{ik}{4\pi}e^{q_0}Ei(-q_0) + \frac{ia_3}{4\pi}e^{q_3}Ei(-q_3) + \frac{ia_4}{4\pi}e^{q_4}Ei(-q_4) \quad \text{(A5)}$$

Here Ei is the complex exponential integral, which is obtainable from tabulations or convenient series representations. Also $q_0 = k(2D + ix)$, $q_1 = S_1(2D + ix)$, $q_2 = -S_2(2D + ix)$, $q_3 = -S_3(2D - ix)$, $q_4 = -S_4(2D - ix)$, while the a_n and S_n are elementary functions of k and the free-surface parameter $kF^2 \equiv \omega U/g$ and are listed in the references.

The first line in Eq. (A5) represents the kernel without a free surface. The first term of the second line is the image for $F \gg 1$. All the remaining terms describe a system of wave trains, one associated with the wake and the rest propagating at various speeds relative to the hydrofoil. When $kF^2 = \frac{1}{4}$ (cf. Figs. 6–8), infinite loading is experienced, according to

linearized theory, because two of the trains are shifting over from the forward to the rearward direction of relative propagation.

Equation (A4) is solved by chordwise collocation, using only the θ terms in the series of Eq. (10).

Free Surface Effect in Three Dimensions at Arbitrary Froude Number

Again the integral equation can be written as in Eq. (8). After considerable effort, it has proved possible to express the kernel function for a planar hydrofoil parallel to the surface as follows:

$$K = K_\infty + K_{3D} \tag{A6}$$

$$K_{3D}(x_0, y_0;\ k, D, F) = 2\frac{\partial}{\partial z}\int_0^\infty K_{2DFS}\left[x_0 + \lambda y_0;\ k, D(1+\lambda^2)^{1/2}, \frac{F}{(1+\lambda^2)^{1/4}}\right]d\lambda + 2\frac{\partial}{\partial z}\int_0^\infty K_{2DFS}\left[x_0 - \lambda y_0; k, D(1+\lambda^2)^{1/2},\ \frac{F}{(1+\lambda^2)^{1/4}}\right]d\lambda \tag{A7}$$

Here K_∞ is the kernel for infinite depth. $x_0 \equiv x - \xi$ and $y_0 \equiv y - \eta$, as before. K_{2DFS} denotes the free-surface portion of the two-dimensional kernel from Eq. (A5), i.e., everything but the first line. The differentiation with respect to z means that K_{2DFS} is to be written first for an arbitrary value of z, the derivative is then taken, and finally $z \to 0$.

The convenience of Eq. (A7) is that wave propagation behavior in K_{2D} has already been fully investigated. Moreover, the integrals may be interpreted as describing a summation of two-dimensional wave trains, λ being the tangent of the angle between the propagation direction and the x axis.

Once the foregoing result is accessible, it is not difficult to generalize to three-dimensional doublet sheets representing nonplanar surfaces. No sample computations have been done because of limited available machine time, and because it is felt that important problems of dynamic loading and hydroelastic stability will usually occur at high enough F to permit simple imaging.

Apparent Mass of Submerged Plates

If a nearly plane plate S executes small normal motions $\Delta z(x, y, t)$ in an unbounded volume of liquid at rest at infinity, the noncirculatory loading can again be simulated with a sheet of ψ doublets over S. Because of the simpler relationship between φ and ψ when $U = 0$, the derivation of the following integral equation and kernel function is quite straightforward:

$$\Delta z = \frac{1}{4\pi}\iint_S \frac{\Delta p}{p_\infty} K_{VM} d\xi d\eta \tag{A8}$$

$$K_{VM} = \lim_{z\to 0}\left\{\frac{\partial^2}{\partial z^2}\left(\frac{1}{R}\right)\right\} = -\frac{1}{[(x-\xi)^2 + (y-\eta)^2]^{3/2}} \tag{A9}$$

Arbitrary time dependence is included, and the double dot denotes two differentiations with respect to time.

Numerical solution of Eq. (A8) calls for replacing Eq. (10) with a series that implies zero bound circulation but causes Δp to be infinite all around the periphery of S. This can be accomplished by substituting $\csc\theta$ for $\cot\theta/2$. The principal-value integration differs from the forward-motion case in that only the triple pole at $\xi = x$, $\eta = y$ has to be isolated. Extension to a nonplanar plate is elementary, and free-surface effect can be handled with an antisymmetrical image whenever $\omega^2 l/g \gg 1$.

References

[1] Jones, R. T. and Cohen, D., "High speed wing theory," *General Theory of High Speed Aerodynamics* (Princeton University Press, Princeton, N. J., 1954), Vol. VI, Sec. A.

[2] Ward, G. N., *Linearized Theory of High Speed Flow* (Cambridge University Press, London, 1955).

[3] Heaslet, M. A. and Lomax, H., "Supersonic and transonic small perturbation theory," *General Theory of High Speed Aerodynamics* (Princeton University Press, Princeton, N. J., 1954), Vol. VI, Sec. D, Chap. 5.

[4] Ferrari, C., "Interaction problems," *Aerodynamic Components of Aircraft at High Speeds* (Princeton University Press, Princeton, N. J., 1957), Vol. VII, Sec. C.

[5] Watkins, C. E., Runyan, H. L., and Woolston, D. S., "On the kernel function of the integral equation relating the lift and downwash distributions of oscillating finite wings at subsonic speeds," NACA Rept. 1234 (1955).

[6] Garrick, I. E. and Rubinow, S. I., "Theoretical study of air forces on an oscillating or steady thin wing in a supersonic main stream," NACA TN 1383 (1947).

[7] Kaplun, S. and Lagerstrom, P., "Asymptotic expansions of Navier-Stokes solutions for small Reynolds numbers," J. Math. Mech. **5**, 585 (1957); also Lagerstrom, P., J. Math. Mech. **5** (1957).

[8] Landahl, M. T., Ashley, H., and Widnall, S., "Some free surface effects on unsteady hydrodynamic loads and hydroelasticity," Fourth Symposium Naval Hydrodynamics, Office of Naval Research, ACR-92, pp. 527–549 (1964).

[9] Widnall, S. and Landahl, M. T., "Digital calculation of steady and oscillatory hydrofoil loads including free surface effects," *Proceedings of the International Symposium on Analogue and Digital Techniques Applied to Aeronautics* (to be published).

[10] Ashley, H., "Some recent developments in interference theory for aeronautical applications," *Proceedings of the Sixth Symposium of the Division of Fluid Mechanics, Polish Academy of Science;* also Massachusetts Institute of Technology Fluid Dynamics Research Laboratory Rept. 63-3 (July 1963).

[11] Pines, S., Dugundji, J., and Neuringer, J., "Aerodynamic flutter derivatives for a flexible wing with supersonic and subsonic edges," J. Aeronaut. Sci. **22**, 693–700 (1955).

[12] Johnson, L. G. and Andrew, L. V., "B-70 wing-tip interference program: supersonic box method," North American Aviation, Inc., Rept. SID 61-300 (October 1961).

[13] Watkins, C. E., Woolston, D. S., and Cunningham, H. J., "A systematic kernel function procedure for determining aerodynamic forces on oscillating or steady finite wings at subsonic speeds," NASA Rept. R-48 (1959).

[14] Hsu, R. T., "Some recent developments in flutter analysis of low-aspect-ratio wings," *Proceedings of the IAS National Specialists Meeting on Dynamics and Aeroelasticity* (Institute of Aerospace Sciences, New York, 1958), pp. 7–26.

[15] Stark, V. J. E., "Aerodynamic forces on rectangular wings oscillating in subsonic flow," Saab TN 44, Saab Aircraft Co. (1960).

[16] Cunningham, H. J. and Woolston, D. S., "Developments in the flutter analysis of general plan form wings using unsteady air forces from the kernel function procedure," *Proceedings of the IAS National Specialists Meeting on Dynamics and Aeroelasticity* (Institute of Aerospace Sciences, New York, 1958), pp. 27–36.

[17] Saunders, G. H., "Aerodynamic characteristics of wings in ground proximity," Master of Science Thesis, Dept. of Aeronautics and Astronautics, Massachusetts Institute of Technology (1963).

[18] Crimi, P. and Statler, I. H., "Forces and moments on an oscillating hydrofoil," Fourth Symposium Naval Hydrodynamics, Office of Naval Research, ACR-92, pp. 477–494 (1964).

[19] Zartarian, G. and Hsu, P. T., "Theoretical studies on the prediction of unsteady supersonic airloads on elastic wings," Parts I and II, Wright Air Development Center TR 56-97 (1955, 1956).

[20] Ashley, H., "Supersonic airloads on interfering lifting surfaces by aerodynamic influence coefficient theory," The Boeing Co., Rept. D2-22067 (1962).

[21] Peterson, R. H., "The effects of wing-tip droop on the aerodynamic characteristics of a delta-wing aircraft at supersonic speeds," NASA Tech. Memo. X-363 (1960); title unclassified.

[22] Landahl, M. T., *Unsteady Transonic Flow* (Pergamon Press, London, 1961).

[23] Miles, J. W., *The Potential Theory of Unsteady Supersonic Flow* (Cambridge University Press, Cambridge, England, 1959).

[24] Thwaites, B. (ed.), *Incompressible Aerodynamics* (Clarendon Press, Oxford, England, 1960).

[25] Woods, L. C., *The Theory of Subsonic Plane Flow* (Cambridge University Press, Cambridge, England, 1961).

[26] Greidanus, J. H., van de Vooren, A. I., and Bergh, H., "Experimental determination of the aerodynamic coefficients of an oscillating wing in incompressible, two-dimensional flow," Parts I–IV, National Luchvaart-laboratorium, Amsterdam, Repts. F-101–F-104 (1952).

[27] Ransleben, G. E., Jr. and Abramson, H. N., "Experimental determination of oscillatory lift and moment distributions on fully submerged flexible hydrofoils," Southwest Research Institute, Rept. 2, Contract No. Nonr-3335 (00) (1962).

[28] George, M. B. T., "A theoretical approach to the problem of stall flutter," Contract AF33(038), Cornell Univ. Graduate School of Aeronautical Engineering (1953).

[29] Miller, R. H., "Unsteady airloads on helicopter rotor blades," Fourth Cierva Memorial Lecture, The Royal Aeronautical Society (October 1963).

[30] Miller, R. H., "On the computation of airloads acting on rotor blades in forward flight," J. Am. Helicopter Soc. **7**, 56–66 (April 1962).

[31] Smith, A. M. O. and Pierce, J., "Exact solution of the Neumann problem. Calculation of non-circulatory plane and axially symmetric flows about or within arbitrary boundaries," Douglas Aircraft Co., Inc., Rept. ES 26988 (1958).

[32] Hess, J. L., "Comparison of experimental pressure distributions with those calculated by the Neumann program," Douglas Aircraft Co., Inc., Rept. ES 29813 (1960).

[33] Smith, A. M. O., "Incompressible flow about bodies of arbitrary shape," IAS Paper 62-143 (June 1962).

[34] Rubbert, P. E., "Theoretical characteristics of arbitrary wings by a non-planar vortex lattice method," The Boeing Co., Rept. D6-9244 (1962).

[35] Rubbert, P. E., "Two dimensional airfoils in ground effect," The Boeing Co., Rept. D6-8117 (1962).

[36] Davenport, F. J., "Singularity solutions to general potential-flow airfoil problems," The Boeing Co., Rept. D6-7202 (May 1963).

[37] Kussner, H. G. and von Gorup, G., "Instationäre linearisierte Theorie der Flügelprofile endlicher Dicke in inkompressibler Strömung," Mitteilungen aus dem Max Planck Inst. für Strömungsforschung und der Aerodynamische Versuchsanstalt, Göttingen no. 26 (1960).

[38] van de Vooren, A. I. and van de Vel, H., "Unsteady profile theory in incompressible flow," Rept. TW-17, Mathematisch Institut, Rijksuniversiteit, Groningen, The Netherlands (June 1963).

[39] Lighthill, M. J., "Higher approximations in aerodynamic theory," *General Theory of High Speed Aerodynamics* (Princeton University Press, Princeton, N. J., 1954), Vol. VI, Sec. E.

[40] Spreiter, J. R. and Alksne, A. Y., "Thin airfoil theory based on approximate solution of the transonic flow equation," NACA Rept. 1359 (1958).

[41] Clarke, J. H. and Wallace, J., "Uniform second-order solution for supersonic flow over delta wing using reverse-flow integral method," Division of Engineering, Brown Univ., Rept. CM-1034 (April 1963).

[42] Covert, E. E., "The aerodynamics of distorted surfaces," *Proceedings of the Symposium on Aerothermoelasticity*, U. S. Air Force Aeronautical Systems Div., Rept. 61-645, pp. 369–406 (1961).

[43] Landahl, M. T., "Linearized theory for unsteady transonic flow," *UTIAM Symposium Transsonicam* (Springer Verlag, Berlin/Göthingen/Heidelberg, 1964), pp. 412–439; also Massachusetts Institute of Technology, Fluid Dynamics Research Lab. Rept. 63-2 (March 1963).

[44] Landahl, M. T., "Approximate solution for an oscillating source in a non-uniform transonic stream," North American Aviation, Inc., Rept. SID 63-1194 (August 1963).